ELSEVIER

Polymer 43 (2002) 6505–6514

polymer

www.elsevier.com/locate/polymer

Fracture toughness of α- and β-phase polypropylene homopolymers and random- and block-copolymers

H.B. Chen[a], J. Karger-Kocsis[b,*], J.S. Wu[a], J. Varga[c]

[a]*Department of Mechanical Engineering, Hong Kong University of Science and Technology, Clear Water Bay, Hong Kong, People's Republic of China*
[b]*Institut für Verbundwerkstoffe GmbH, Universität Kaiserslautern, P.O. Box 3049, D-67653 Kaiserslautern, Germany*
[c]*Department of Plastics and Rubber Technology, Budapest University of Technology and Economics, H-1521 Budapest, Hungary*

Received 9 May 2002; received in revised form 13 August 2002; accepted 15 August 2002

Abstract

The fracture and failure mode of α- and β-phase polypropylene homopolymers (PP-H), block- (PP-B) and random-type (PP-R) copolymers with ethylene were studied in high speed (1.2 m/s) flexural tests and compared. The crystallinity of the α- and β-modifications was assessed by wide-angle X-ray scattering and differential scanning calorimetry. The linear elastic fracture mechanical parameters, viz. fracture toughness (K_c) and fracture energy (G_c), were determined at room temperature and $T = -40$ °C on notched Charpy specimens. β-Phase PP-H and PP-B showed superior toughness to the α-versions. On the other hand, K_c and G_c were similar for PP-R in the temperature range studied for both α- and β-modifications. Fracture surfaces of the broken specimens were inspected in scanning electron microscopy and the related failure mode concluded. A model was proposed to explain the toughness improvement via β-crystallinity by considering all proved experimental findings. © 2002 Published by Elsevier Science Ltd.

Keywords: α-Polypropylene; β-Polypropylene; Polypropylene copolymers

1. Introduction

β-Nucleated isotactic polypropylene homopolymers (PP-H) have received considerable interest recently. This interest is mostly due to the peculiar thermal and mechanical performance of the β-crystalline PP-H [1–3]. The toughness of β-phase PP-H is markedly higher than that of the α-modification, both below and above the glass transition temperature (T_g). This has been demonstrated in several works adopting the methods of linear [4–6] and elasto-plastic fracture mechanics [7–10]. Note that fracture mechanics is the right tool when a toughness comparison between various PP modifications is targeted. Concepts of the fracture mechanics, in fact, may yield an inherent material parameter which is independent of the test configuration. Attention should be paid to the fact that a break-thorough in the research and application of β-crystalline PPs occurred when highly selective β-nucleants became available [1,3,11].

Interestingly, the mechanisms of toughness improvement are still the topic of intense debates [5,7,10]. There are no doubts, however, about the role of the microstructure (lamellar ordering) and loading-induced β–α polymorphic transition. Therefore the dispute is focused on which are the causes and consequences of the toughness enhancement and how to distinguish between them. The most comprehensive review on β-phase PPs by Varga [1] highlights that the effect of β-crystallinity on the toughness of random- (PP-R) and block-type PP copolymers (PP-B) was less studied [12–15]. Further, authors of the related works have used non-selective β-nucleants with the only exception of Zhang and Shi [12]. In addition, for the toughness determination of rubber-toughened PPs (PP melt blended by rubbers) only Grein et al. [15] used fracture mechanical methods. By contrast, the melting and crystallization characteristics of β-nucleated PP-R and PP-B systems have been well explored. It was shown that PP-R has a reduced tendency to β-crystallization [2,16,17].

Therefore the aim of this paper was to determine the fracture mechanical parameters of β-crystalline PP-R and PP-B systems produced by highly selective β-nucleants and to compare the related values with those of the α-modifications. In order to get a more complete picture,

* Corresponding author. Fax: +49-631-2017-199.
E-mail address: karger@ivw.uni-kl.de (J. Karger-Kocsis).

0032-3861/02/$ - see front matter © 2002 Published by Elsevier Science Ltd.
PII: S0032-3861(02)00590-6

Table 1
Basic properties of the PPs involved in this study

Designation	Grade	Producer	M_n (kg/mol)	M_w (kg/mol)	Ethylene content (%)	MFI (dg/min)[a]
PP-H (α)	Daplen BE 50	PCD	150	1000	–	0.3
PP-H (β	Daplen BE 50 (grau)	(Now Borealis) Linz, Austria	150	1000	–	0.3
PP-B[b]	Tipplen K392	Tisza Chemical Works, Tiszaújváros, Hungary	52	207	8–11	12
PP-R	Tipplen R351		52	220	1.8–2.6	12

[a] MFI (melt flow index) determined at $T = 230$ °C with 2.16 kg load.
[b] End block-copolymer type.

the work was extended also for α- and β-phase PP-Hs of extremely high molecular weight (MW). It is worth noting that the toughness improvement through β-crystallinity augments with increasing MW of the PP-H resin [1,18,19]. A further aim of this study was to assess the failure mode by fractography and thus to contribute to some open questions related to the toughness improvement caused by β-crystallinity.

2. Experimental

2.1. Specimens and their characteristics

The basic properties of PP-H, PP-B and PP-R are listed in Table 1. The characteristics of the PPs in Table 1 already indicate that the fracture response of the PP-B and PP-R systems can only be compared with each other. There are some other aspects (β-nucleant, specimen preparation) besides the MW (cf. Table 1) due to which the fracture behavior of the α- and β-phase PP-Hs should be treated separately. On the other hand, a common discussion is straightforward as the polymorphic composition of all PPs involved in this work is known (see below).

α- and β-phase PP-Hs were produced from commercially available grades (cf. Table 1). Note that the β-nucleant in Daplen BE 50 grau is of quinacridone type. This material was used in a recent study in order to clarify the effects of injection molding conditions on the microstructure–property relationships [20]. Plaques ($140 \times 240 \times 4$ mm^3, thickness) were produced from the PP-Hs by hot pressing adopting a special crystallization/annealing procedure (termed $3 \times \beta$) [21].

The β-nucleant used to produce β-phase PP-B and PP-R was a proprietary calcium pimelate compound [1,3]. It was added to the related granules in 0.1 wt% and incorporated by extrusion blending. In order to set the same 'prehistory' for the control α-phase samples, the virgin PP-B and PP-R were also passed through the extruder at the same processing conditions and pelletized. Film-gated plaques (length × width × thickness = $70 \times 140 \times 4$ mm^3) were produced by injection molding from the pellets. These plaques were molded on an Engel ES 200/50 HL type reciprocating screw injection molding machine as reported earlier [19]. The melt temperature, injection speed, mold temperature and holding pressure were set for 240 °C, 70 mm/s, 80 °C and 300 bar, respectively.

Presence of β-phase and the overall crystallinity of the PPs were detected by wide-angle X-ray scattering (WAXS) and differential scanning calorimetry (DSC). WAXS patterns were taken by a Philips goniometer (type PW 1830) using Ni-filtered Cu Kα radiation in the $2\Theta = 5, \ldots, 45°$ with steps of 0.05°. DSC traces were taken by a DSC 821e device (Mettler-Toledo) at 20 °C/min heating rate. In order to demonstrate the difference between the α- and β-modifications, the first heating scan ($T = -100, \ldots, 200$ °C) was followed by a cooling one to $T = 110$ °C, prior to a second heating cycle to $T = 200$ °C. Recall that in this way the thermally induced β–α-recrystallization can be avoided in β-PPs [1–3] and thus a reliable DSC crystallinity can be derived. Our aim was to compare the WAXS and DSC crystallinities and thus to conclude the most probable melt enthalpy for the 100% crystalline β-PP (for which different data are published in the literature).

2.2. Fracture mechanical testing

Rectangular bars of $70 \times 10 \times 4$ mm^3 dimension (length × width (W) × thickness (B)) were sawn from the plaques and notched. In case of the injection-molded plaques, the bars were taken parallel to the mold flow direction (i.e. their notching direction was perpendicular to the mold flow direction). Notching was produced by a Notchvis device of Ceast.

Fracture toughness (critical stress intensity factor, K_c) and fracture energy (critical strain energy release rate, G_c) were determined in high-speed three point-bending (flexural) tests on v-notched specimens. The notch depth (a) was set in the range of a/W (notch length/specimen width) = 0.2–0.8. Prior to testing the v-notch was sharpened by razor blade tapping. The notched Charpy bars were impacted without cushioning on an instrumented impact pendulum of Ceast, equipped with an AFS MK3 data acquisition unit at $v = 1.2$ m/s at room temperature (RT) and $T = -40$ °C, respectively. PP-Hs were also tested at $T = 0$ and -20 °C. Impacting of the specimens occurred under the following conditions: mass of the striker, 2.19 kg; striker working range, 0.55 kN; testing time, up to 8 ms (data sampling interval of 2 μs). The related software

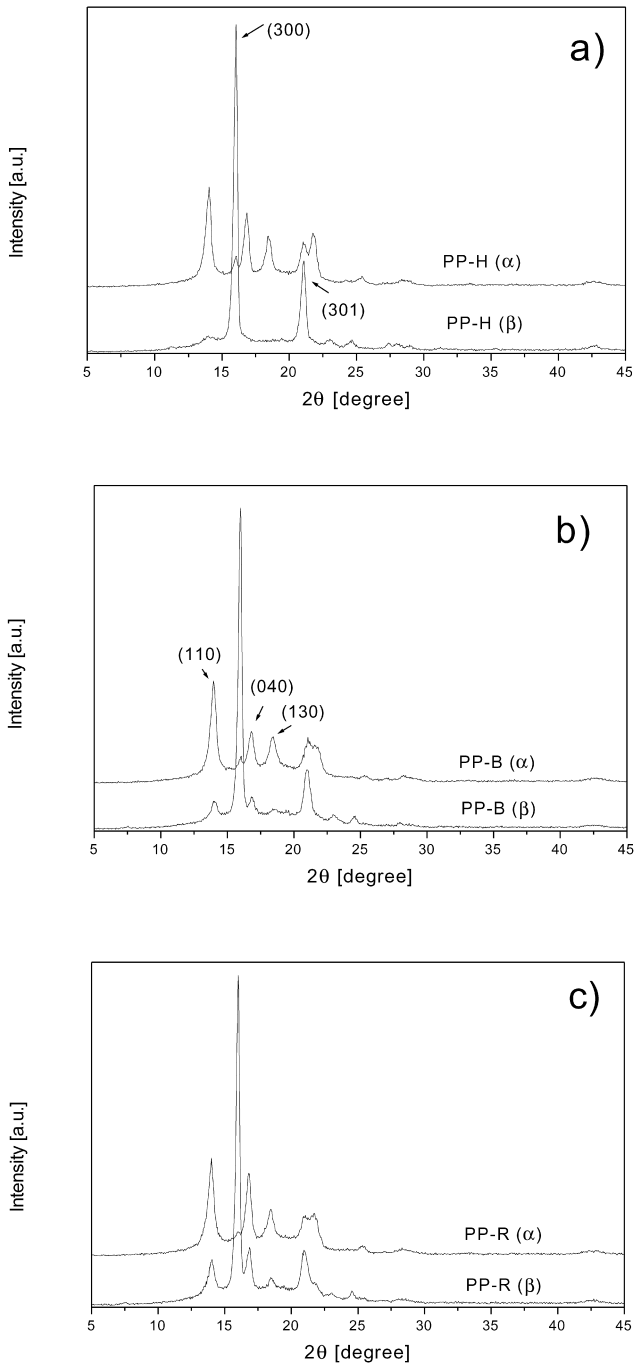

Fig. 1. WAXS patterns for the α- and β-crystalline PP-H (a), PP-B (b) and PP-R (c). Note: characteristic β-peaks are marked by arrows.

allowed us to display the fracture history as a function of time or deflection. According to the fractograms which registered the maximum load (F_{max}), the energy absorbed up to F_{max} (energy required for fracture initiation, E_{init}) and the full energy absorbed (E_{total}) were read or computed. For K_c (based on F_{max}) and G_c (based on E_{init}) determination the recommendations of the ESIS TC-4 group [22] were adopted. In respect to G_c, this approach agrees with that of Plati and Williams [23]. It should be noted that G_c was read from the slope of E_{init} vs. BWϕ (where ϕ is the shape

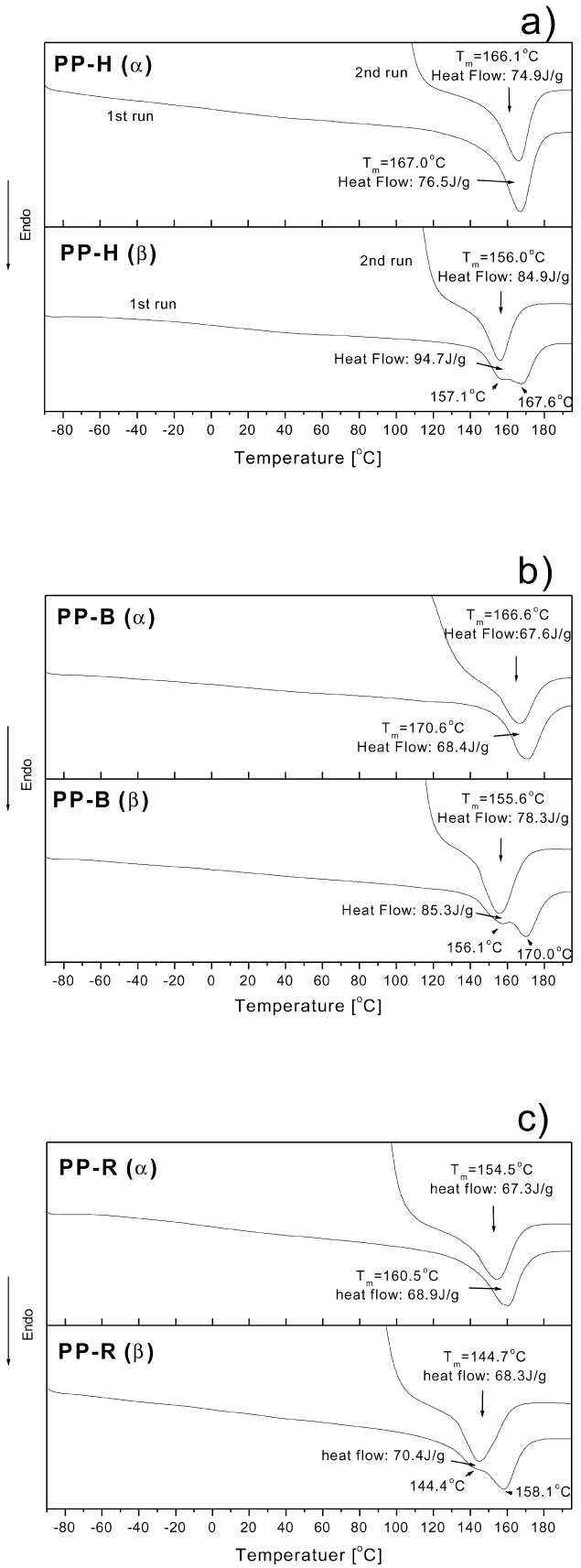

Fig. 2. DSC heating traces (first and second heating runs, respectively) for the α- and β-crystalline PP-H (a), PP-B (b) and PP-R (c).

Table 2
Crystallinity data of the PPs concluded from WAXS and DSC measurements

Samples	Modification	WAXS				DSC		
		K	X_c	X_c (β)	X_c (α)	Melting enthalpy (J/g)	X_c (β)	X_c (α)
PP-H	α	0.124	0.45	0.06	0.39	75	–	0.42
	β	0.949	0.51	0.48	0.03	84	0.50	–
PP-B	α	0.123	0.40	0.05	0.35	68	–	0.38
	β	0.788	0.50	0.39	0.11	78	0.46	–
PP-R	α	0.100	0.38	0.04	0.34	67	–	0.38
	β	0.707	0.48	0.34	0.14	68	0.40	–

Note: DSC α- and β-crystallinity were determined by accepting 177.0 and 168.5 J/g for the 100% crystalline α- and β-modifications, respectively [25].

factor depending on the specimen and testing configuration [22,23]) passing the origin of the coordinate system. This, however, did not practically differ from the related value taken as the slope of the linear regression using the experimental data. The correlation coefficient of the G_c values was never below 0.90. K_c and G_c data included in this paper represent mean values of 5 and 15 measurements performed on specimens of the same ($a/W \sim 0.5$ for K_c determination) and of varying a/W ratios (for G_c assessment), respectively.

2.3. Fractography

The fracture surface of the broken specimens was analyzed in a scanning electron microscope (SEM; Jeol JSM 5400) after gold coating.

3. Results and discussion

3.1. α- and β-crystallinity

Fig. 1 shows the WAXS patterns for the α- and β-crystalline PPs studied. The intense peak at $2\Theta = 16.2°$ and the less intense one at $2\Theta = 21°$ are assigned to the 300 and 301 planes of the β-crystals. The peak at 16.2° is widely used to detect the β-content of the polymorphous PP via the K-value of Turner Jones et al. [24]:

$$K = \frac{I_{(300)\beta}}{I_{(300)\beta} + I_{(110)\alpha} + I_{(040)\alpha} + I_{(130)\alpha}} \quad (1)$$

Accordingly, $K = 1$ for the fully β- and 0 for the fully α-crystalline PP. The overall crystallinity (X_c) was determined by:

$$X_c = \frac{A_c}{A_c + A_a} \quad (2)$$

where A_c and A_a are the areas under the crystalline peaks and amorphous halo, respectively. The β-crystallinity is given by KX_c, whereas for the α-crystallinity $X_c - KX_c$ holds. The crystallinity values derived from the WAXS measurements are summarized in Table 2.

Characteristic DSC traces (first and second heating) are displayed in Fig. 2. The βα-recrystallization during the first run is well-resolved for the β-modifications (cf. shoulder on or doubling of the melting peak). As expected, the second heating for β-crystalline PPs does not yield any melt peak doubling. One can also notice that the melting of the β-phase occurs at a somewhat lower temperature than that of α-modification. This is in agreement with the literature

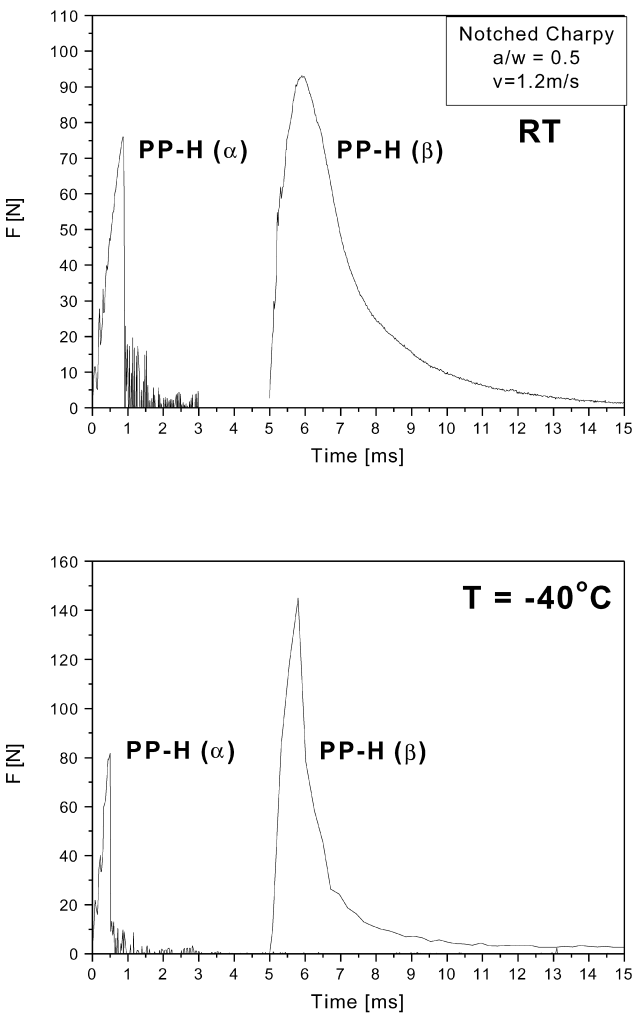

Fig. 3. Characteristic force–time traces due to impact of the notched Charpy specimens ($a/W = 0.5$) at room temperature (RT) and $T = -40$ °C for the α- and β-modifications of PP-H.

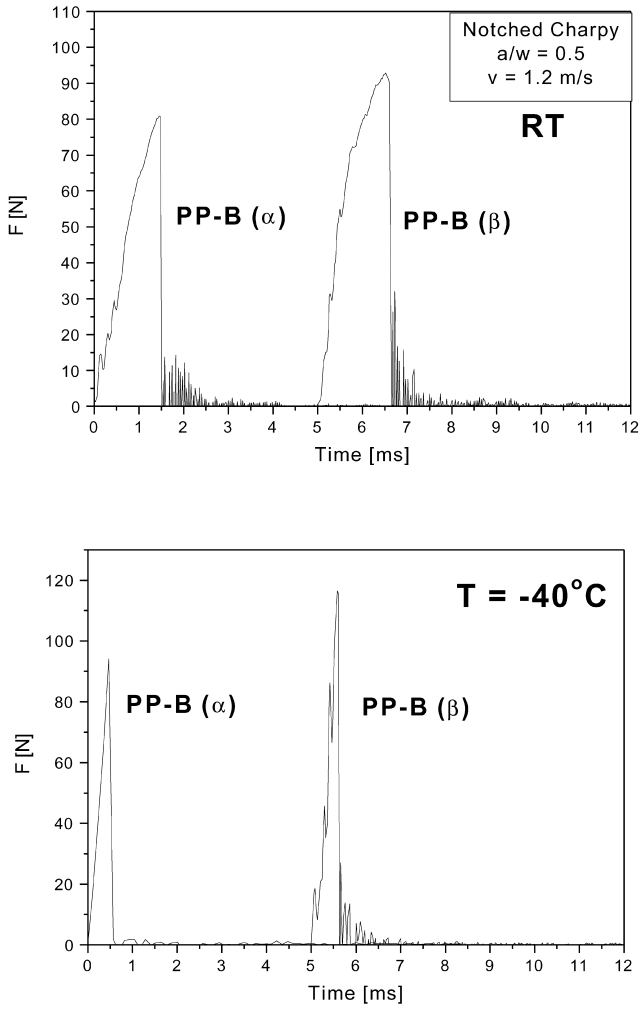

Fig. 4. Characteristic force–time traces due to impact of the notched Charpy specimens ($a/W = 0.5$) at room temperature (RT) and $T = -40$ °C for the α- and β-modifications of PP-B.

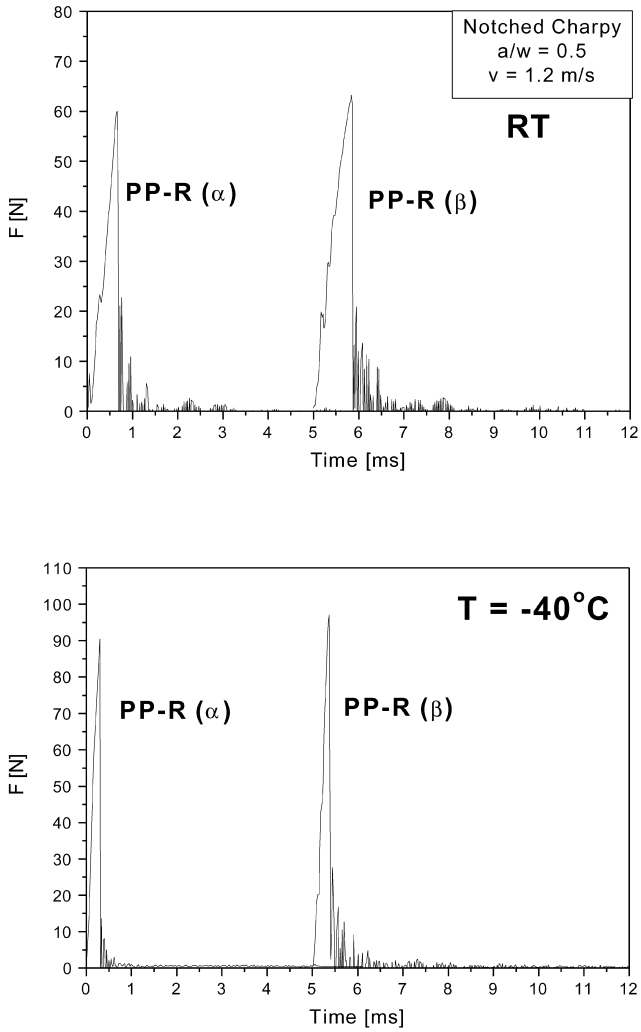

Fig. 5. Characteristic force–time traces due to impact of the notched Charpy specimens ($a/W = 0.5$) at room temperature (RT) and $T = -40$ °C for the α- and β-modifications of PP-R.

[1–3]. The lack of the βα-recrystallization during the second heating run allows us to determine the melt enthalpy of the β-phase (cf. Table 2). Table 2 also contains the melt enthalpy values of the α-modifications. The best agreement between the WAXS and DSC results can be achieved when 177.0 and 168.5 J/g are accepted for the 100% crystalline α- and β-phase PP, respectively. These values were proposed recently by Li et al. [25]. It is worth noting that both WAXS and DSC data in Table 2 are deduced from one measurement each.

3.2. Fracture mechanics

Characteristic force–time traces registered during fracture of the notched Charpy specimens at comparable a/W ratio (ca. 0.5) as a function of crystalline modification and temperature are depicted for PP-H, PP-B and PP-R in Figs. 3–5, respectively. The α-modifications of all PPs impacted at both temperatures showed typical brittle fracture (cf. Figs. 3–5). The related fractograms are of a triangular shape with a lack of crack propagation in the postmaximum range. This failure mode prevailed in the β-phase PP-R at both RT and $T = -40$ °C (cf. Fig. 5) and even in the β-phase PP-B at $T = -40$ °C (cf. Fig. 4). The fractogram of the β-phase PP-B at RT (cf. curved appearance of the related force–time trace in Fig. 4) suggests the onset of some short range ligament yielding. This should be associated with the development of a discernible plastic zone. Crack propagation after the maximum load can only be detected for the β-modified PP-H (cf. Fig. 3). This finding is in harmony with earlier results achieved on rather high MW β-modified PPs [5]. It should be stressed here that the fractograms—except those of β-phase PP-Hs—clearly support our working hypothesis, viz. the linear elastic fracture mechanics can be used to describe the fracture response of PPs at high speed impact. As the fracture toughness, K_c, correlates with the load [22]:

$$K_c = f\frac{F_{max}}{BW^{1/2}} \quad (3)$$

Table 3
Fracture mechanical data (K_c, G_c) as a function of crystalline modification and testing temperature for the PPs studied

Sample	Modification	K_c (MPa m$^{1/2}$)				G_c (kJ/m^2)			
		$T = -40$ °C	−20 °C	0 °C	RT	−40 °C	−20 °C	0 °C	RT
PP-H	α	2.4	2.6	2.5	2.2	1.8	2.0	2.1	6.2
	β	4.2	4.2	3.8	2.6	5.7	6.0	5.9	9.3
PP-B	α	2.4	–	–	2.2	2.1	–	–	6.2
	β	3.1	–	–	2.5	3.9	–	–	11.4
PP-R	α	2.3	–	–	1.7	2.3	–	–	3.2
	β	2.6	–	–	1.7	2.0	–	–	2.5

Designation:- not measured.

where f is the shape factor and all other parameters have been defined earlier, one can get the first impression of how K_c is changing with the temperature and crystalline modification. Accordingly, K_c experiences a slight decrease as a function of temperature for all PPs studied. This is in line with the expectation for a thermoplastic polymer, the T_g of which is covered by the temperature range set. A marked difference in the K_c values can only be observed between the α- and β-modifications of PP-H and PP-B. K_c is always higher for the β- than for the α-modification (cf. Table 3).

Recall that the fracture energy, G_c, is given by Refs. [22,23]:

$$G_c = \frac{E_{init}}{BW\phi} \tag{4}$$

As E_{init} is the energy absorbed up to F_{max} and the fracture time changes linearly with the deflection in the first approximation, the related surface below the force–time traces hints at G_c. Considering the fractograms in Figs. 3–5, one can expect a large change in G_c as a function of crystalline modification and temperature for PP-B and especially for PP-H. On the other hand, G_c is likely unaffected by either the testing temperature or the polymorphy for the PP-R (cf. Fig. 5). The related G_c data in Table 3 support this prediction. A drop in K_c and a steep increase in G_c can be found at RT for PP-H and PP-B, i.e. just above the T_g of PP. This behavior is often referred to as brittle/ductile transition. Before further discussion, it seems appropriate to collate the data in Table 3 with those already published. Such a comparison under dynamic conditions can only be done for PP-H, as fracture mechanical data for PP-B and PP-R are missing. Results from a recent work performed on 15 vol% rubber-toughened PP [15] can, however, be considered when discussing the fracture behavior of PP-B (containing ca. 10 vol% rubber—cf. Table 1). The K_c and G_c values reported for injection-molded α- and β-phase PP-Hs [5] are lower than the present ones. The fact that the MW and K-value (cf. Eq. (1)) of the PP-H in Ref. [5] were markedly lower and similar, respectively, to the present grade, suggests a great influence of the molding-induced skin-core morphology and core spherulitic structure. Similar, but somewhat, lower K_c and G_c data were published for injection-molded α- and β-phase PP-Hs by Nezbedova et al. [6] and Tjong et al. [4,26]. The K-values of the P-Hs in the cited works were ca. 0.6 and 0.9, respectively. The dynamic fracture energy of injection-molded β-phase PP-Hs of very low K-values [27] lay considerably below our present data. The K_c and G_c data of injection-molded rubber-toughened PP-Hs are comparable with ours at a similar impact speed [15]. Albeit the MW, β-crystallinity and other morphological parameters are less disclosed in the cited papers, the above brief summary on the dynamic fracture mechanical parameters already indicates how complex the toughness–structure relationship is. It was outlined recently that the toughness of semicrystalline polymers depends on molecular (MW, tie molecule density) and supermolecular characteristics (crystallinity, spherulite size, skin-core structure) in a very complex way [28,29]. This aspect will be discussed later in respect to the failure mode of β-nucleated PP.

3.3. Fractography

The fracture surface of the α- and β-phase PP-Hs are rather similar at RT which is in concert with the related G_c data (cf. Table 3). Comparing the fracture surfaces of the α- and β-phase PP-Hs at $T = -40$ °C (cf. Fig. 6a and b) one can recognize that the β-form produced a more 'patchy' appearance. This is the result of microvoiding (accompanied by crazing) which occurred during fracture and resulted in a threefold increase in G_c (cf. Table 3). There is some hint that the craze-like structure was broken via thermal fracture (arrow indicates in Fig. 6b). Remnants caused by thermal fracture became more discernible at high magnifications.

The fracture surface of the α- and β-phase PP-B at $T = -40$ °C is quite similar (Fig. 7). Near to the notch the boundary, the initially formed plastic zone can well be resolved (broken line indicates the crack tip blunting front in Fig. 7b. A similar but smaller plastic zone can also be observed in Fig. 7a). Fig. 8 is a high magnification SEM picture taken of the transition zone between the plastic zone and the fast fracture region. One can clearly see that the rubbery particles in the plastic zone of PP-B introduce multiple crazing (which is likely preceded by cavitation)

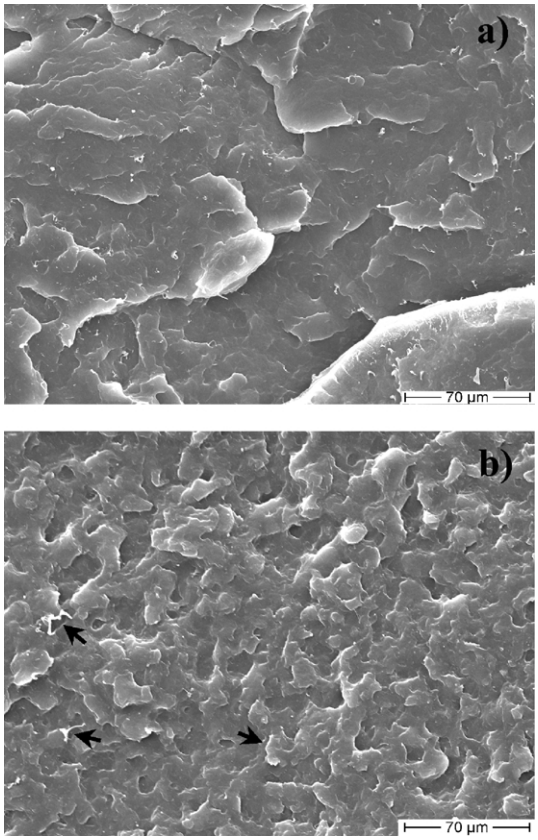

Fig. 6. SEM microphotographs taken of the fracture surface of α- (a) and β-phase (b) PP-H specimens broken at $T = -40\,^{\circ}C$. Note: arrows in (b) indicate thermal fracture.

and the crazes break up later on by fast fracture. Note that crystallization in both PP-B and PP-R results in a fine dispersion of rubbery (ethylene–propylene based) particles. Their primary function is to alleviate the triaxial stress state and transform it into a two-dimensional one. Fig. 8 also shows that the particle size of the rubbery domains is quite broad. The toughness data in Table 3 along with the SEM results (cf. Figs. 7 and 8) indicate that the fracture mode and thus the absorbed energy in PP-B are governed by both rubber dispersion and β-crystalline modification.

The failure of PP-R is completely different from PP-B at β-crystallinity. SEM pictures taken in the fast fracture range (Fig. 9a) show a very fine, uniform distribution of the rubber inclusions in the α-phase PP-R. They should act as usual impact modifiers in PPs. Interestingly, these rubber particles can hardly be resolved on the fracture surface of β-phase PP-R (cf. Fig. 9b). As the K_c and G_c values of the α- and β-phase PP-Rs are similar and the rubbery-phase is not present on the fracture surface of β-PP-R one can conclude that the effects of rubber dispersion (in case of α-PP-R) has been 'overwritten' by that of the β-crystallinity (in β-PP-R) without yielding, however, any toughness improvement. This peculiarity may be traced to the low ethylene and thus low rubber content of the PP-R used. Considering the fact that the toughness of β-phase PP-H (even at comparable

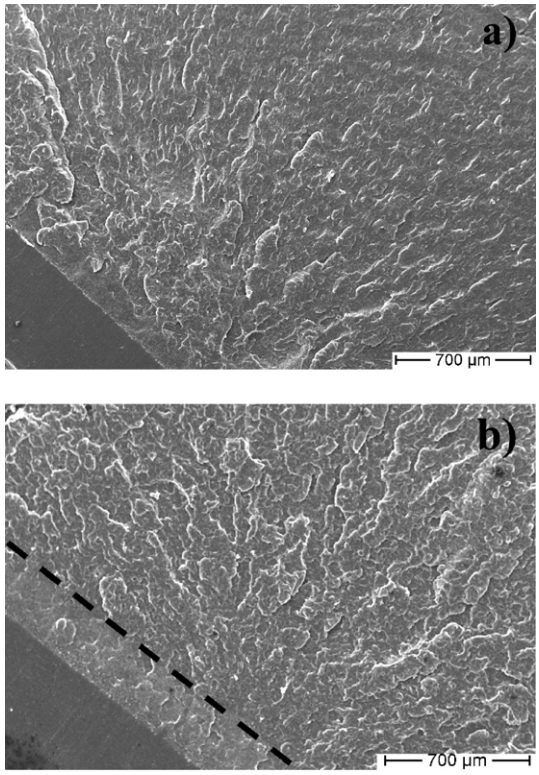

Fig. 7. SEM microphotographs taken of the fracture surface of α- (a) and β-phase (b) PP-B specimens broken at $T = -40\,^{\circ}C$. Note: broken line shows the boundary of the plastic zone in (b).

MW) is similar or superior to α-phase PP-R (Table 3), the latter can be replaced by β-phase PP-H. Thus, this replacement can be done without any property penalty, as has been shown on the example of extruded pipes [30].

3.4. Effects of β-crystallinity

As mentioned already in Section 1, there are several explanations for the toughness improving effect of β-crystallinity. In order to settle this issue, first we have to list the most important experimental findings.

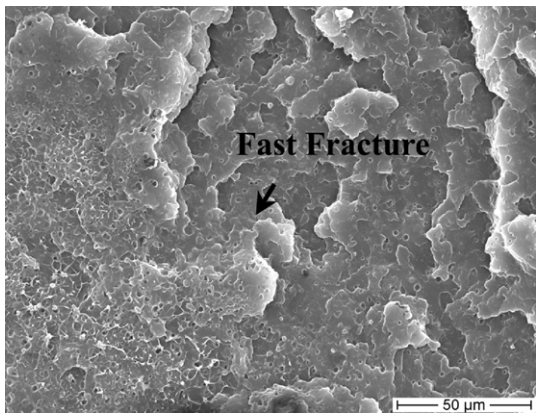

Fig. 8. High-magnification SEM pictures taken of the fracture surface of β-phase PP-B after fracture at $T = -40\,^{\circ}C$.

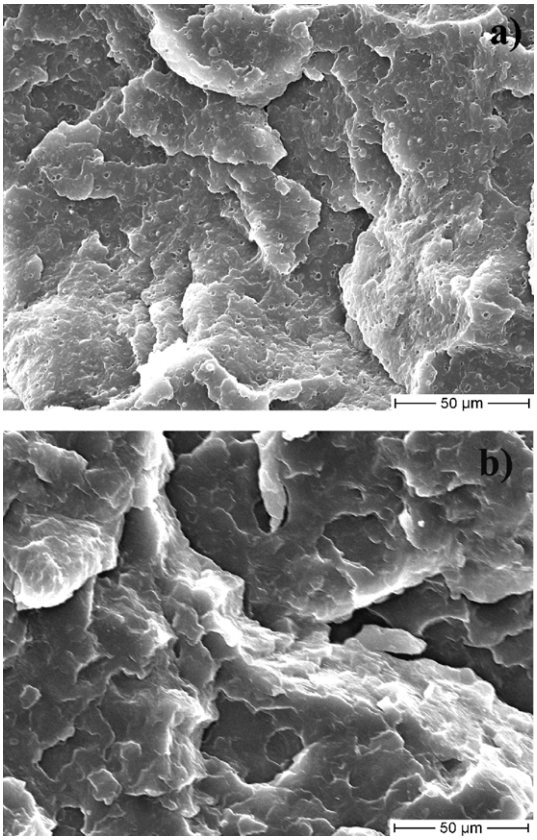

Fig. 9. SEM microphotographs taken of the fracture surface of α- (a) and β-phase (b) PP-R specimens broken at $T = -40$ °C.

3.4.1. Molecular weight

It has already been shown in numerous papers that increasing MW (or decreasing MFI) results in improved toughness for β-nucleated PPs [18,19,31]. It should, however, be emphasized that an MW increase simultaneously causes a strong enhancement in the tie molecules density [28,29]. Unfortunately, the latter aspect in PP was never studied in detail.

3.4.2. β-Crystallinity/β-nucleant

High β-crystallinity (high K-value according to Eq. (1)) usually yields high toughness [27,32]. However, very high β-crystallinity can be achieved in low MW PP-Hs [18,31] the toughness of which is moderate (see above). Comparing the fracture response of β-nucleated PPs (cf. [5]), one can claim that the more selective the β-nucleant, the higher the toughness improvement.

3.4.3. β-Phase morphology (lamellar structure)

This aspect is again of paramount importance. It was demonstrated by several authors that β-lamellae are not organized in a cross-hatched but in a bundled structure [33–36]. Recall that the cross-hatched structure is characteristic for the α-lamellae [2]. The bundled β lamellar structure exhibits an inherently higher ductility than the cross-hatched one. Attention should be paid to the fact that even the structure of the β-lamellae is very complex (branching on screw dislocations, three-dimensional curvatures [1,37]). Nevertheless, lamellae bundles, held together by the tie molecules, can easy separate from one another upon loading. This lamellae separation is accompanied by massive voiding with the simultaneous onset of a craze like microporous structure [34–36,38]. Needless to say that the high MW and thus high tie molecules density strongly favor the formation of this microporous structure [38]. It is also worth mentioning that the production of films with such a microporous structure is one of the preferred applications of β-phase PP [1,39]. The lamellae involved in this craze-network deform and break-up by homogeneous (tilting) and heterogeneous slippages (break-up) [34,40]. Those lamellae which are oriented along the loading direction may defold. This failure, viz. break-up and defolding of the lamellae, triggers the β–α polymorphic transition. This occurs via a recrystallization process as the handedness of the helices in the related elementary cells should change during this transition [1–3]. This transition also represents an energy sink which is a further contribution to toughness improvement. This β–α transition should happen also in the early stage of the lamellae separation process, namely in those curved, bent sections of the lamellae which are under high local bending or tensile stresses. Transmission electron microscopy (TEM) combined with focused electron diffractography should give the lacking evidence for this. Note that the mechanical loading-induced β–α transition seems to be a gradual process (i.e. the β-to-α conversion increases with increasing strain) based on some papers [2,7,30,31,41]. One should not forget, however, the fact that most techniques used to detect the β–α transition were sensitive for bulk, and never for a single lamella. This β-to-α transition is associated with volume contraction by considering the densities of the related elementary cells [7]. Since the specimen volume does not relax during loading, the β–α transition should amplify the microvoiding process. Massive microvoiding/crazing means that the triaxial stress state prevailing in the specimen is becoming a biaxial one (in fracture mechanical terms this is a transition from plane strain toward plane stress). Thus, this transition enhances the toughness per se. Recall that this transition in the stress state is often quoted as the major argument for the toughness improvement in impact modified polymers of both thermoplastic and -setting nature [42]. The proposed failure scenario, considering the above failure events, is depicted schematically in Fig. 10.

Based on Fig. 10 one could get the impression that the scheme in Fig. 10 is valid only for low strain tests and only above the T_g of PP. On the other hand, it was shown also in this paper, that β-phase PP-H exhibits higher toughness than the α-counterpart even below T_g and also at high strain rates (i.e. due to impact). The sketch in Fig. 10 holds also for this case. The only difference is that voiding/crazing through lamellae separation are suppressed. Instead of this, the β–α transition and accompanied voiding dominate. The

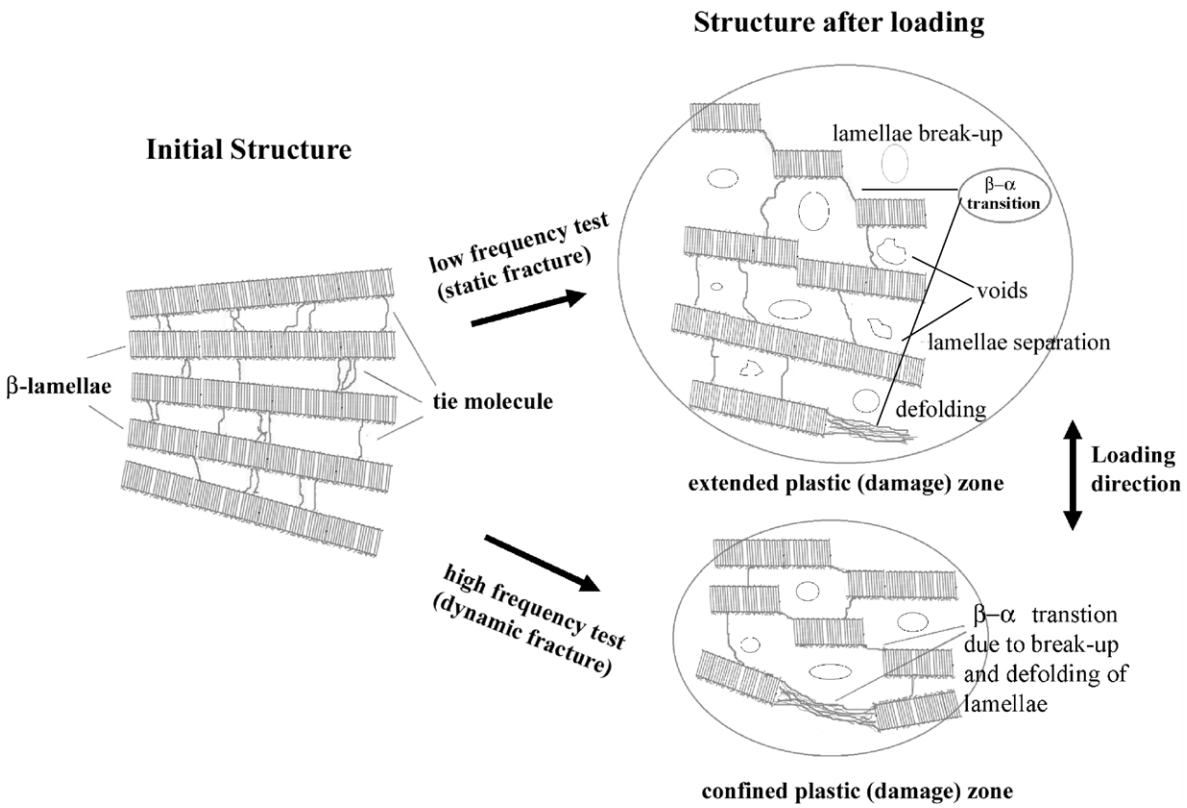

Fig. 10. Scheme of the failure mode of β-crystalline PP at low and high strain rates (frequencies), respectively.

onset of the β–α transition has been demonstrated in several works devoted to the dynamic fracture behavior of β-phase PP-H [5,31]. Summing up the above failure mode the authors would like to underline that the above control parameters were already mentioned, however, not so explicitly, in an earlier work of Karger-Kocsis et al. [5].

4. Conclusions

Based on this work performed on the fracture mechanical characterization of α- and β-crystalline PP homopolymers (PP-H), block (PP-B) and random copolymers (PP-R), the following conclusions can be drawn:

(i) β-Crystallinity strongly increases the toughness of PP-H and PP-B both below and above T_g.
(ii) β-Crystallinity may suppress the effect of rubber dispersion in PP-R, however, without affecting the overall toughness response. This finding holds likely for tests both below and above T_g.
(iii) The energy absorbing mechanisms triggered by the β-modification were identified. The proposed failure model considers all relevant experimental results. Accordingly, the major material-related parameters which yield high toughness in a β-phase PP are: MW and tie molecules density (stabilization and extension of a crazed/voided network), lamellar arrangement (efficient stress transfer and stress relief) and β–α-phase transition (additional energy absorption due to recrystallization and local 'hardening' of the micro-porous network). The relative occurrence of the related failure mechanisms changes as a function of testing frequency (strain rate) and temperature.

Acknowledgements

This work was supported by the DAAD, through sponsoring the research stay of H.B. Chen. J. Varga acknowledges the support of the Hungarian Scientific Foundation (OTKA:T-034230).

References

[1] Varga J. J Macromol Sci Phys 2002;B41: 1121–71.
[2] Varga J. In: Karger-Kocsis J, editor. Polypropylene: structure, blends and composites, vol. 1. London: Chapman & Hall; 1995. p. 56. chapter 3.
[3] Varga J, Ehrenstein GW. In: Karger-Kocsis J, editor. Polypropylene: an A–Z reference. Dordrecht: Kluwer; 1999. p. 51.
[4] Tjong SC, Shen JS, Li RKY. Scr Metall Mater 1995;33:503–8.
[5] Karger-Kocsis J, Varga J, Ehrenstein GW. J Appl Polym Sci 1997;64: 2057–66.
[6] Nezbedova E, Pospisil V, Bohaty P, Vlach B. Macromol Symp 2001; 170:349–57.
[7] Karger-Kocsis J. Polym Engng Sci 1996;36:203–10.

[8] Karger-Kocsis J, Varga J. J Appl Polym Sci 1996;62:291–300.
[9] Tordjeman Ph, Robert C, Marin G, Gerard P. Eur Phys J E 2001;4:459–65.
[10] Labour T, Vigier G, Séguéla R, Gauthier C, Orange G, Bomal Y. J Polym Sci B: Polym Phys 2002;40:31–42.
[11] Varga J, Mudra I, Ehrenstein GW. J Appl Polym Sci 1999;74:2357–68.
[12] Zhang X, Shi G. Polymer 1994;35:5067–72.
[13] Sterzynski T, Lambla M, Crozier H, Thomas M. Adv Polym Technol 1994;13:25–36.
[14] Fujiyama M. Int Polym Process 1998;13:291–8.
[15] Grein C, Plummer CJG, Kausch H-H, Germain Y, Béguelin Ph. Polymer 2002;43:3279–93.
[16] Varga J, Schulek-Tóth F. J Thermal Anal 1996;47:941–55.
[17] Juhász P, Varga J, Belina K, Belina G. J Macromol Sci Phys 2002; B41: 1173–89.
[18] Fujiyama M. Int Polym Process 1995;10:251–4.
[19] Karger-Kocsis J, Moos E, Mudra I, Varga J. J Macromol Sci Phys 1999;B38:647–62.
[20] Varga J, Breining A, Ehrenstein GW, Bodor G. Int Polym Process 1999;14:358–64.
[21] Varga J, Tóth F. Macromol Chem Macromol Symp 1986;5:213–23.
[22] Pavan A. In: Moore DR, Pavan A, Williams JG, editors. Fracture mechanics testing methods for polymers adhesives and composites. ESIS Publication 28. Oxford: Elsevier, 2001, p. 27.
[23] Plati E, Williams JG. Polym Engng Sci 1975;15:470–7.
[24] Turner Jones A, Aizlewood JM, Beckett DR. Makromol Chem 1964;75:134–54.
[25] Li JX, Cheung WL, Jia D. Polymer 1999;40:1219–22.
[26] Cheung T, Tjong SC, Li RKY. SPE-ANTEC 1996;54:2256–9.
[27] Raab M, Kotek J, Baldrian J, Grellmann W. J Appl Polym Sci 1998;69:2255–9.
[28] Karger-Kocsis J. Macromol Symp 1999;143:185–205.
[29] Karger-Kocsis J. In: Cunha AM, Fakirov S, editors. Structure development during polymer processing. NATO series E, vol. 370. Dordrecht: Kluwer 2000, p. 163.
[30] Karger-Kocsis J, Putnoki I, Schöpf A. Plast Rubber Compos Process Appl 1997;26:372–5.
[31] Karger-Kocsis J, Mouzakis DE, Ehrenstein GW, Varga J. J Appl Polym Sci 1999;73:1205–14.
[32] Fujiyama M. Int Polym Process 1995;10:172–8.
[33] Tjong SC, Shen JS, Li RKY. Polymer 1996;37:2309–16.
[34] Coulon G, Castelein G, G'Sell C. Polymer 1999;40:95–110.
[35] Li JX, Cheung WL, Chan CM. Polymer 1999;40:2089–102.
[36] Li JX, Cheung WL, Chan CM. Polymer 1999;40:3641–56.
[37] Trifonova D, Varga J, Ehrenstein GW, Vancso GJ. J Polym Sci B: Polym Phys 2000;38:672–81.
[38] Karger-Kocsis J. In preparation.
[39] Chu F, Yamaoka T, Kimura Y. Polymer 1995;36:2523–30.
[40] Karger-Kocsis J. Polym Bull 1996;36:119–24.
[41] Riekel C, Karger-Kocsis J. Polymer 1999;40:541–5.
[42] Paul DR, Bucknall CB, editors. Polymer blends. New York: Wiley; 2000.